Interferometric noise characterization of a 2-D time-spreading wavelength-hopping OCDMA network using FBG encoding and decoding

Craig Michie,[1,*] Ivan Andonovic,[1] R. Atkinson,[1] Yanhua Deng,[2] Jakub Szefer,[3] Camille-Sophie Bres,[2] Yue Kai Huang,[2] Ivan Glesk,[2] Paul Prucnal,[2] Kensuke Sasaki,[4] and Gyaneshwar Gupta[4]

[1]*Department of Electronic and Electrical Engineering, University of Strathclyde, Glasgow, Scotland G1 1XW*
[2]*Department of Electrical Engineering, Princeton University, Princeton, New Jersey 08544, USA*
[3]*Department of Electrical and Computer Engineering, University of Illinois at Urbana-Champaign, Urbana, Illinois 61801, USA*
[4]*Oki Electric Industry Company Ltd., Corporate Research and Development Centre, Hachiouji-shi, Tokyo 193-8550, Japan*
[*]*Corresponding author: c.michie@eee.strath.ac.uk*

Received November 2, 2006; revised February 8, 2007; accepted March 15, 2007; published May 15, 2007 (Doc. ID 76693)

The results of a range of experimental characterization exercises of interferometric noise for the case of a representative 2-D time-spreading wavelength-hopping optical code family are presented. Interferometric noise is evaluated at a data rate of 2.5 Gbits/s within an OCDMA network emulation test bed established utilizing fiber Bragg grating encoders/decoders. The results demonstrate that this form of noise introduces significant system power penalties and must be taken into consideration in any OCDMA network designs and implementations.

OCIS codes: 060.0060, 060.2330, 060.4230.

1. Introduction

Optical code-division multiple access (OCDMA) is a system approach able to support bursty, variable data rate traffic with a reduced network management overhead. The performance of OCDMA systems at the physical layer is limited by a combination of noise sources, the more critical being multiple-access interference (MAI) and interferometric noise (IN). IN occurs when same (delayed replica) or different optical signals with identical, or very close, frequencies are incident simultaneously on the same photodetector. Due to the square-law photodetector characteristic, all the incident signals beat and the photocurrent attributed to IN is much greater than that owing to the incident optical power of the cross-talk signal alone. Therefore, more severe system performance degradation and error floors result [1–3]. Most optical systems are prone to IN, for example, wavelength division multiplexing (WDM) [4,5], time-division multiplexing (TDM) [6,7], subcarrier multiplexing [8,9], and OCDMA [10–22].

IN can be classified according to the origin of both data and cross-talk signals; single or distinct optical sources. When both data and cross talk originate from the same laser source, the delay time due to multiple paths is the key parameter. According to the relation between the coherence time of the laser source and the differential delay between source and detector (τ), three classes of IN arise [2].

If the delay is much smaller than the coherence time, the interference is very close to the coherence limit, i.e., *coherent cross talk*. In such a case, laser phase noise is not a factor, and IN may arise due to environmental phase noise (e.g., temperature variation). *Incoherent cross talk*, on the other hand, also called phase-induced intensity noise (PIIN), occurs when the delay is much greater than the coherence time. In such a case, noise results from the conversion of the laser phase noise into intensity noise [2]. The impact of coherent and incoherent cross talk has been studied extensively, and higher-power penalties are attributed to incoherent cross talk. The intermediate region representing the third class where both the delay and coherence time are com-

parable is referred to as *partially coherent cross talk*. The resulting noise is very difficult to analyze and depends on the exact value of $\omega\tau$; where ω is the angular frequency. Although these classes have been discussed extensively theoretically and experimentally for a variety of WDM and subcarrier multiplexing scenarios, they have not been rigorously studied yet for OCDMA systems.

The second classification layer characterizes IN where data and cross-talk signals originate from distinct laser sources. Two cases are considered depending on the relation between the beat frequency of the signals, f, and the receiver electrical bandwidth, B_e. If the beat frequency falls within the receiver bandwidth ($f \ll B_e$), the IN case occurs and the phase noise is converted into high levels of intensity noise by in-band optical mixing. When the beat frequency is greater than the receiver bandwidth ($f \gg B_e$), IN *free noise* case occurs (out of band). Electronic filtering limits the beat noise leaving only the additive cross talk. The main scope of this experimental characterization concerns only the case of IN.

The first study of beat noise in OCDMA systems was performed for spectral amplitude coding (SAC) schemes employing broadband optical sources [10]. Subsequently, several studies have considered beat noise in estimating the performance of different OCDMA systems; frequency encoding (FE) [10–12], frequency hopping (FH) [13], sequence-inversion keyed (SIK) [14], and coherence multiplexing (CM) [15]. Generally, the level of beat noise is found to be proportional to the square of light intensity multiplied by the ratio of the electrical to optical bandwidth. For coherent optical sources, limited research is found considering the effect of IN; note that the strategies of deriving the IN for incoherent and coherent optical sources are different. The impact of IN has been investigated for 1-D time spreading [16] and 2-D time-wavelength (TW) OCDMA [17–20]. Recently, an experimental study contrasting coherent and incoherent noise sources has been reported demonstrating the performance of four users at 1.25 Gbits/s under the influence of IN [21]. An error floor at 10^{-9} occurred with four users at a received power of −2 dBm. This paper presents the initial experimental characterization of the level of beat noise for 2-D optical codes under a number of interference conditions. It is best viewed as a framework of experimental data, which supports the development of theoretical models describing more extensive networks based on OCDMA.

1.A. Two-Dimensional Time-Spreading Wavelength-Hopping Codes (2-D TW)

Of the many optical code families developed thus far, from a theoretical perspective based on the correlation properties of the codes, 2-D (TW) optical CDMA systems appear to be a potentially promising technique for network implementations supporting a high number of simultaneous subscribers [23,24]. A range of 2-D codes has been reported, most readily classified into two main categories; single pulse per row or column (SPPR/C) or multiple pulse per row or column (MPPR/C);. Prime hop, modified prime hop (MPH), carrier-hopping prime (CHP), prime/optical orthogonal codes (OOC), and asymmetric prime hop are representative of SPPR/C while the latter category includes an extended carrier-hopping prime (ECPHC). In 2-D TW codes, selected pulses are encoded in distinct or similar wavelengths according to a certain algorithm. When all the available wavelengths are used and each wavelength appears only once in each code word at different time slots, the code is referred to as symmetric (S) or equivalently SPPR/C. For asymmetric codes (AS), some wavelengths are selected from the wavelength pool for each codeword. If at least two different wavelengths located at the same time slot, the code represents multiple pulse per column (MPPC). Multiple pulse per row (MPPR) codes result if at least one wavelength appears twice (or more). Due to the nature type of the optical domain, the minimum cross correlation between any two codes is "1," producing a hit or line up, i.e., interference between active codes constituting MAI.

Most of the literature has studied the performance of 2-D TW scheme under the MAI-limited case. However, for a more accurate system evaluation as indicated by many other all-optical network analyses, IN must be taken into consideration. There are different sources of unwanted cross-talk signals including cochannel interference (MAI), optical component imperfections, multiple reflections, or fiber nonlinearity. This study will initially focus on the analyses and characterization of beat noise due to the homodyne beating arising from cochannel interference between 2-D TW codes, using this as the basis to extend that framework to consider other impairments.

1.B. Experimental Procedure

The 2-D TW OCDMA network under emulation is a star configuration. At the transmitter, the optical source is modulated according to the user data and the output is encoded in the two dimensions. Bit error rate (BER) measurements were performed on the OCDMA test bed with fiber Bragg gratings (FBGs) used for encoding and decoding the data. The network was designed to support up to four users (four different encoders) sending data and one receiver, comprising a decoder, which was matched to one of the encoders (users). Different communication scenarios were emulated by varying the number of users and by adjusting the individual properties, e.g., polarization or delay of the transmitted user signals. For each scenario, BER measurements were taken in order to quantify the detrimental effect of interferometric noise on the quality (in terms of power penalty) of the selected channel.

Figure 1 is a schematic of the test bed. The light source was a mode-locked supercontinuum (SC) laser. The 12 nm flat SC is generated from the propagation of a 1.6 ps model locked pulse (at a 2.5 GHz repetition rate) from an erbium-doped fiber laser through a dispersion decreasing fiber (DDF). Two pulse streams are produced by a 20/80 splitter, the outputs of which were launched into two polarization insensitive electroabsorption (EA) modulators driven at 2.5 Gbits/s from two independent bit error testers (BERTs) generating uncorrelated $2^{15}-1$ pseudorandom binary sequence (PRBS) sequences. The two main branches represented the "data"—modulated signal for the primary encoder (user), designated spread spectrum user 1 (SPU1)—and the "interferers." The second modulator was used to modulate data signal for the remaining encoders (users), designated SPU4, SPU5, and SPU6. After optical amplification through an erbium-doped fiber amplifier (EDFA), both branch signals were sent to the FBG encoders.

To provide flexibility in the type of network scenarios that the test bed could emulate, each interferer signal (SPU4, SPU5, and SPU6) was passed through a polarization loop controller (PLC) and a tunable optical delay line (TDL) (that is manually controlled). The TDLs were used to adjust the position of the cross-correlation interfering signals in relation to the desired data represented by the autocorrelation peak. The TDLs also allow for adjustment of delays between different users, thus providing the ability to establish various interference conditions. The PLCs control the relative polarization between the cross-correlation and autocorrelation signals, providing the ability to establish the worst case for the generation of beat noise with polarizations aligned and the sum-of-intensities (representative of the more conventional MAI) case with crossed polarizations. After the encoding and conditioning of the signals was performed, all four signals are combined in a 1×4 optical multiplexer, amplified further by an EDFA and transmitted through a short length of optical fiber.

At the receiving end, the combined signals were input to a decoder, also a FBG device designated as SPU2. The decoder is a mirror image of an encoder to which it is paired, i.e., the delays between the reflected wavelengths are inverted, in so doing realigning the wavelengths in the time domain and constructing the autocorrelation peak comprising the incoherent summation of four chips. In this way, signals that are matched with the encoder produce a strong autocorrelation peak, while signals sent with different codes produce cross correlations. Since the receiver decoder is designed to receive SUP1, a cross correlation on all other codes is executed. The test bed was

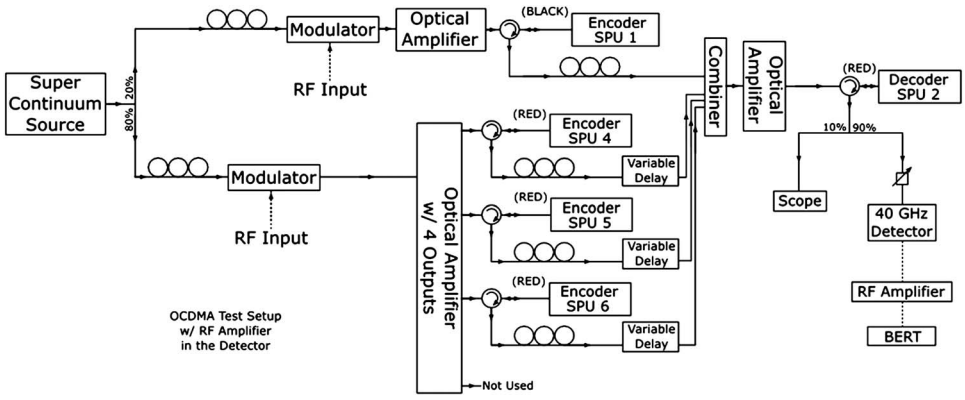

Fig. 1. OCDMA networking test bed.

established to eliminate any coherence effects that may be expected when operating with a single laser source; the coherence of the source was only confined to each successive mode-locked pulse from the laser.

Given the flexibility of the test bed, a set of interference conditions, i.e., overlaps between the autocorrelation peak and various combinations of interfering chips from three other codes as well as between interfering codes can be emulated. Since any one of the cochannel interfering chips will match one of the wavelengths constituting the autocorrelation peak exactly, not only will MAI occur but also beat noise in the incoherent regime will be generated.

The decoded signal was sent to a BERT through an attenuator and detector. The signals were also monitored on a digital sampling oscilloscope (Tektronix CSA8000) through a 30 GHz front-end detector. The optical attenuator controlled the power of the signal and simulated degrading network conditions. A dc 15 GHz receiver from Agilent was used to detect the output.

2. Test Bed Implementation

As an initial characterization of the test bed, power losses were measured across the various elements. An average loss in an FBG encoder was measured to be 15.6 dB. The relatively high loss is to be expected since in this case, the FBG devices are effectively spectrum splicing a wide optical spectrum generated by the SC source. This power loss combines losses due to a combination of the loss in the FBG passband wavelength, loss in the wavelengths outside of the passband, i.e., the reflected wavelengths and loss in the circulator. The losses in the passband are directly dependent on the spectrum of the source. Further path losses in the system were introduced by the polarization controllers (the average loss was 0.22 dB) and in the delay lines (the average loss was 1 dB).

For the purposes of the characterization, the total power of the main data user was set higher in relation to the total power of each interferer. This condition will produce lower levels of interferometric noise power and allow a more extensive series of measurements to be undertaken. The power of the main user (SPU1) was set to be ~3 dB higher than the other simultaneous users on the channel. This enabled the system characterization to be carried out over a greater number of interferers to highlight degradation trends with user count.

Four encoders, designated SPU1, SPU4, SPU5, and SPU6 were utilized in the experiments. Each encoder is composed of four gratings (wavelengths) at different time delays, thereby creating unique codes. The spread time of each bit was 400 ps, the code length was 16, and the four wavelengths utilized were 1552.52, 1551.72, 1550.92, and 1550.12 nm, all falling on the ITU WDM grid at 100 GHz (0.8 nm) spacing. These orthogonal codes were used throughout the experiments. Only one decoder, SPU2, the exact mirror image of SPU1, was used at the receiver.

The chip positions for all four transmitter encoders are summarized in Table 1. The decoder, SPU2, had the exact gratings as SPU1, but with a reversed order of chip positions. An autocorrelation results for a code match, such as SPU1 and SPU2; conversely a cross correlation is produced for any mismatch condition, e.g., SUP4, SUP5, and SUP6 with SUP2. Please note that for the purposes of the experimental characterization, the cross correlation for SUP4 was established to be two-chip coincident,

Table 1. Summary of the Temporal Positions of Each Chip Within the Encoders[a]

	Encoders:					Decoders			
	λ_1	λ_2	λ_3	λ_4		λ_1	λ_2	λ_3	λ_4
SPU1	15	10	5	0	SPU2	0	5	10	15
SPU4	7	0	13	6		Chip position			
SPU5	2	11	0	9					
SPU6	9	6	3	0					
	Chip position								

[a]Chip time slot is 25 ps; code block is 400 ps.

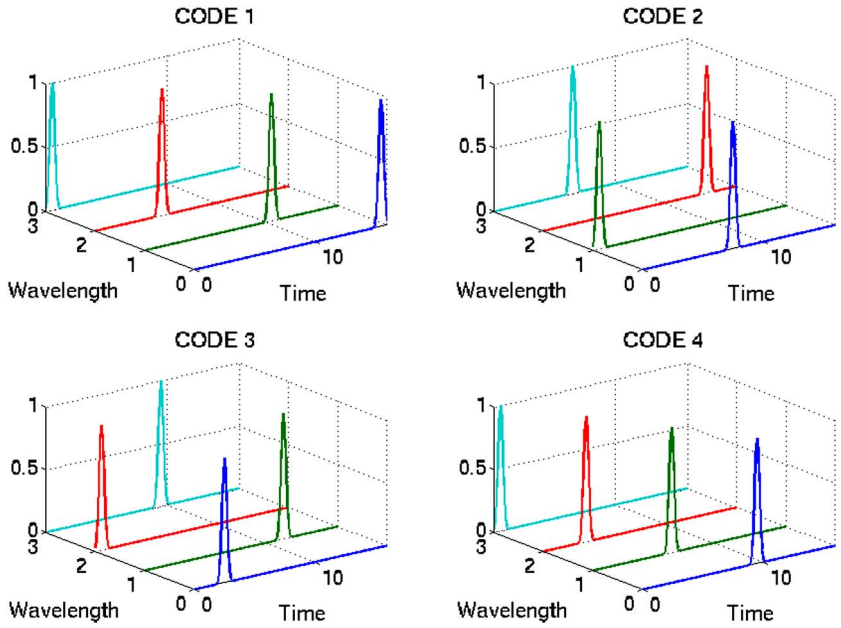

Fig. 2. Visual representation of the four codes produced by the encoders.

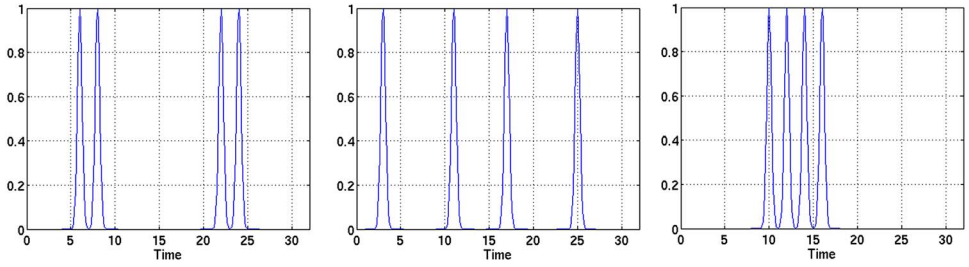

Fig. 3. Simulated cross-correlation outputs for (left) SPU4, (center) SPU5, and (right) SPU6 with SUP2.

facilitating the establishment of a subset of the interference scenarios. Figure 2 is the visualization of these codes in the two dimensions.

Figure 3 shows the simulated (synchronous) cross correlation of SPU2 with SPU4, SPU5, and SPU6. Notice that since the spread length was 31, the designed code block window (equivalent to the data rate) 400 ps, and the code length 16, the spread length is greater than the code length. Therefore when analyzing the observation window, which is equivalent to the code length, overlaps between consecutive chips can occur. For example, the cross correlation generated from SPU4 has chip positions at 7, 5, 23, and 21. In a window length of 16 chips, chips from 7 and 23, 5, and 21, would overlap, thus creating two double-peak pulses. For completeness, the corresponding eye diagram outputs are presented in Fig. 4.

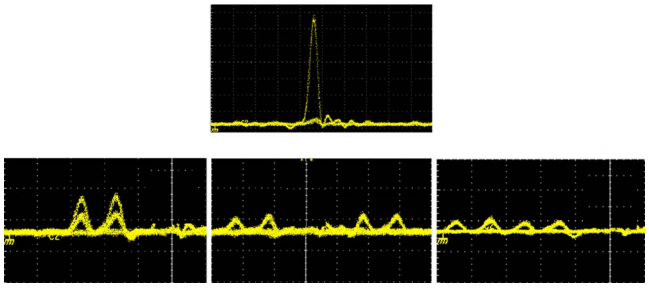

Fig. 4. Output eye diagrams from the receiver depicting the autocorrelation (SUP1, above) and three cross correlation codes: (left) SPU4, (center) SPU5, and (right) SPU6. Please note that the cross correlation for SUP4 was established to be two-chip coincident in order to facilitate the experimentation. The vertical axis is intensity (arbitrary units) and the horizontal axis depicts time (5 ps division).

3. Results

The following results present the BER performance of the emulated OCDMA network under various interference conditions. The aim of the characterization was to determine the trends relating power penalty owing to both MAI and interferometric noise as a function of a range of different networking conditions, e.g., a different number of active users. In all cases, absolute values of power penalty were difficult to obtain due to difficulties in establishing and maintaining polarization state and temporal overlap. This is manifest as errors and variations in the BER trends. In summary, the interference scenarios examined were based upon a single data user in order to establish the "back-to-back reference" against which all other performances would be related:

- Data user plus one interferer with no overlap on the autocorrelation peak.
- Data user plus one interferer with one chip overlap on the autocorrelation peak originating from the cochannel interference of another user.
- Data user plus two interferers with two chips overlapping the autocorrelation peak originating from the cochannel interference of two users.
- Data user plus three interferers with three chips overlapping the autocorrelation peak originating from the cochannel interference of three users.
- Data user with no overlap of the autocorrelation peak from other users but with the overlap of two cross-correlation chips.
- Data user with no overlap of the autocorrelation peak from other users but with the overlap of three cross-correlation chips.

3.A. Single User

The BER as a function of normalized received power for a single user on the network was taken for a total power of −0.4 dBm in code SPU1 and represents the back-to-back measurement subject to minimal noise and the reference performance against which all other scenarios are compared. Shown for reference (Fig. 5) is the optical output waveform (eye diagram) recorded by the oscilloscope; the decoded waveform for the case of only SPU1.

3.B. No Overlap, Two Users

In the one interferer scenarios, two users were present on the network; SPU1 and one other user whose signal interfered with SPU1. The first case examined was with no overlap from a single cochannel user. Figure 6(a) shows the eye diagrams for SPU1 (autocorrelation) with SPU4 (cross correlation) present. Note that the autocorrelation does not overlap with the cross correlation (two side peaks) from SPU4. Figures 6(b) and 6(c) show the equivalent eye diagrams for SPU1/SPU5 and SPU1/SPU6, respectively. The corresponding BER measurement is shown in Fig. 6(d) for the three cases; also shown is the single user performance for reference. This BER was taken for a total power of −0.4 dBm in code SPU1 and approximately −2.5 dBm in SPU4, SPU5,

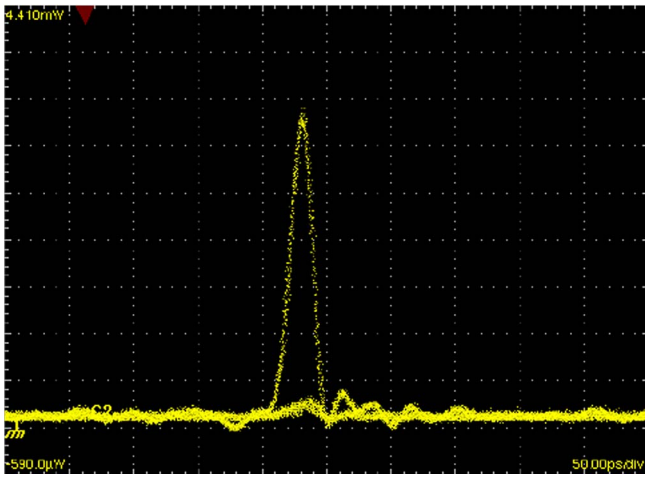

Fig. 5. Eye diagrams from the output of the receiver of the autocorrelation viz. a single user (SPU1).

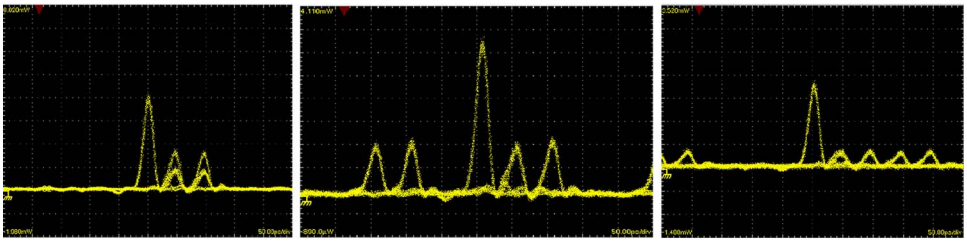

(a) (b) (c)

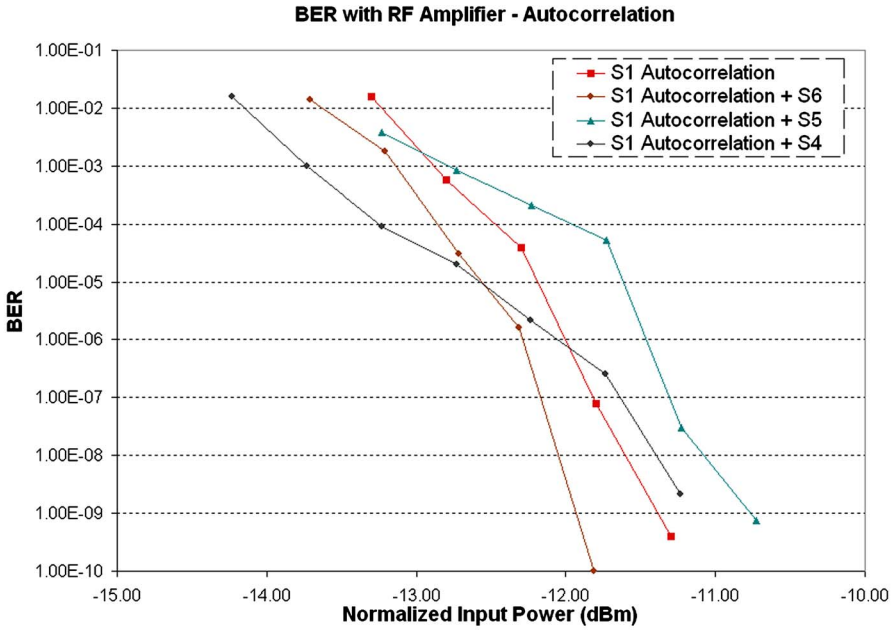

(d)

Fig. 6. Output eye diagrams for the single interferer scenario with no overlap of the autocorrelation peak (a) SPU1 and SPU4, (b) SPU1 and SPU5, (c) SPU1 and SPU6. Note: scales vary. (d) BER, as a function of normalized received power for two users with no direct overlap of the two signals; corresponding to Figs. 9(a)–9(c).

and SPU6. To aid in comparisons, all subsequent BER curves will present the reference case (SPU1 autocorrelation with no interference).

3.C. With Overlap, Two Users

In this single interferer scenario, two users were present; SPU1 and one other whose signal interfered with SPU1 but with one of the cross-correlation chips directly overlapping the autocorrelation peak. Furthermore, through manipulation of the relevant PLCs, the crossed and the aligned polarization states were established to minimize/maximize the beat noise (emulating the MAI case), respectively.

Figure 7 shows the eye diagrams for SPU1 with one cross correlation present, i.e., one of the cross-correlation chips directly overlaps the autocorrelation peak. Figure 7(a) shows the eye diagram for SPU1 with SPU5 with beat noise minimized. Fig. 7(b) shows the eye diagram for SPU1 with SPU5 beat maximized. Similarly Fig. 7(c) shows the eye diagram for SPU1 with SPU6 present, beat noise minimized, and Fig. 7(d) shows the eye diagram for SPU1 with SPU6 present, beat noise maximized. In Figs. 7(b) and 7(d), it is clear that when the polarizations were adjusted to the aligned state, significant levels of beat noise result. The corresponding BER measurements are shown in Fig. 7(e).

3.D. With Overlap, Three Users

In this one interferer scenario, three users were present on the network; SPU1 and two other users whose signal interfered with SPU1. However, only one of the cross-

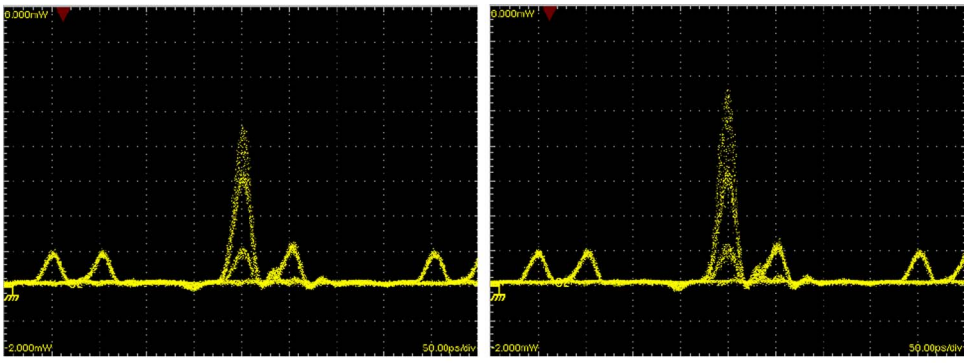

(a) (b)

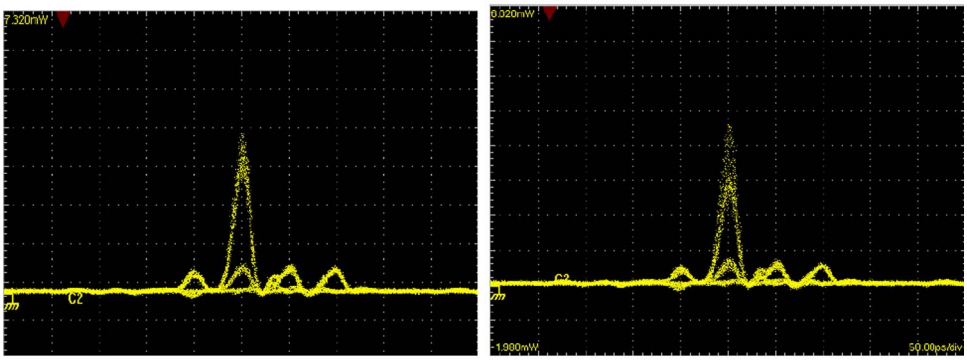

(c) (d)

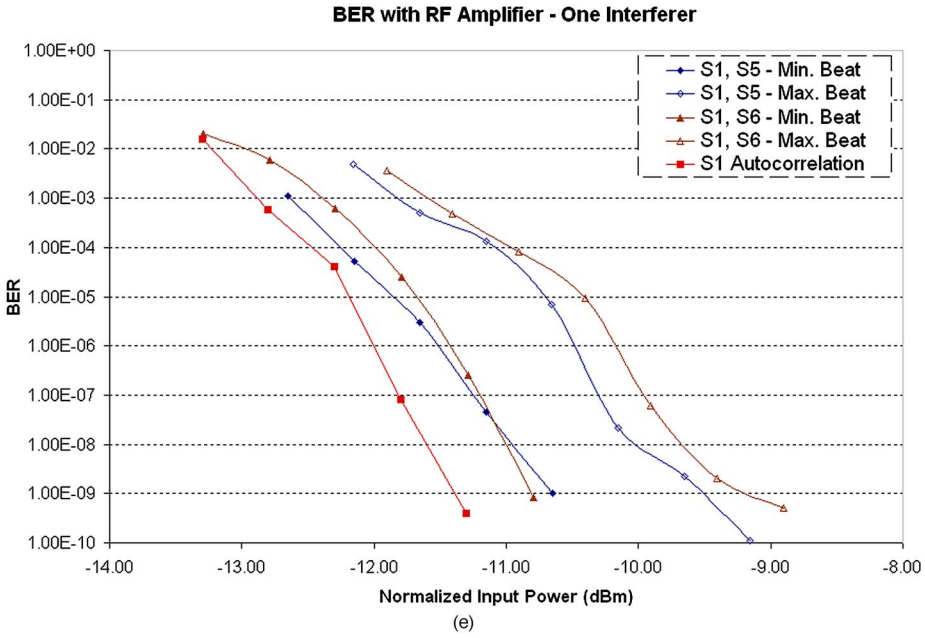

(e)

Fig. 7. Output eye diagrams for the single interferer scenario, two users on the channel, with one-chip overlap of the autocorrelation peak. (a) SPU1 and SPU5 minimized beat noise, (b) SPU1 and SPU5 maximized beat noise, (c) SPU1 and SPU6 minimized beat noise, (d) SPU1 and SPU6 maximized beat noise. (e) BER as a function of normalized received power for two users with direct overlap of a single chip from cochannel interferers SPU5 and SUP6 for minimized/maximized levels of beat noise; corresponding to (a)–(d).

correlation chips directly overlapped the autocorrelation peak while the other, although present, did not directly overlap the autocorrelation peak but nevertheless contributed to cochannel interference.

Figure 8 shows the eye diagrams for SPU1 with two other users present on the channel, i.e., one of the cross-correlation chips directly overlap the autocorrelation

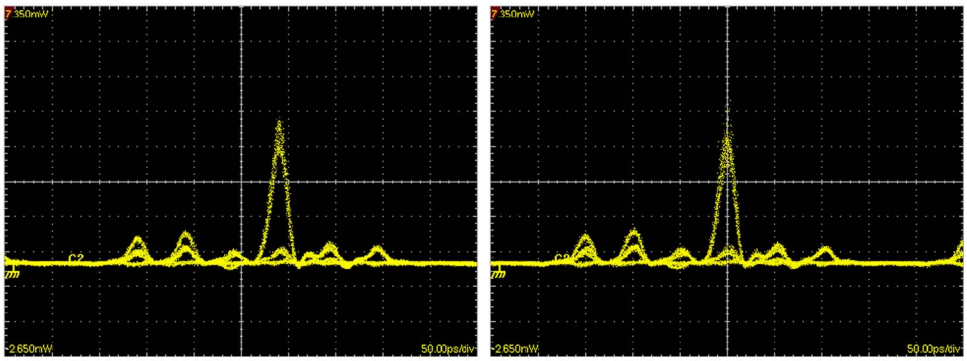

(a) (b)

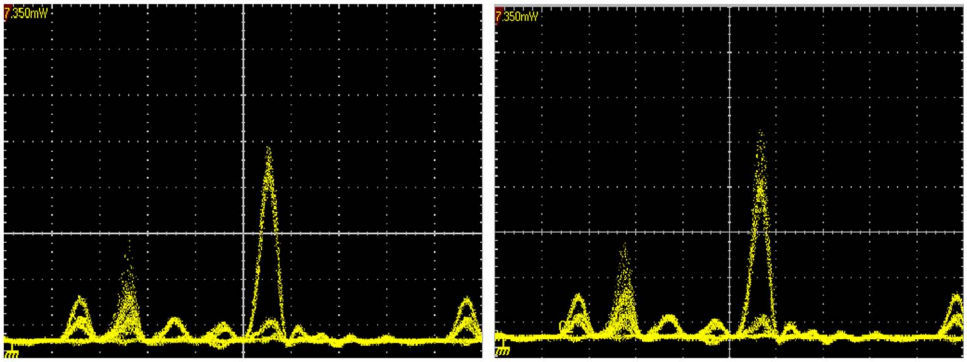

(c) (d)

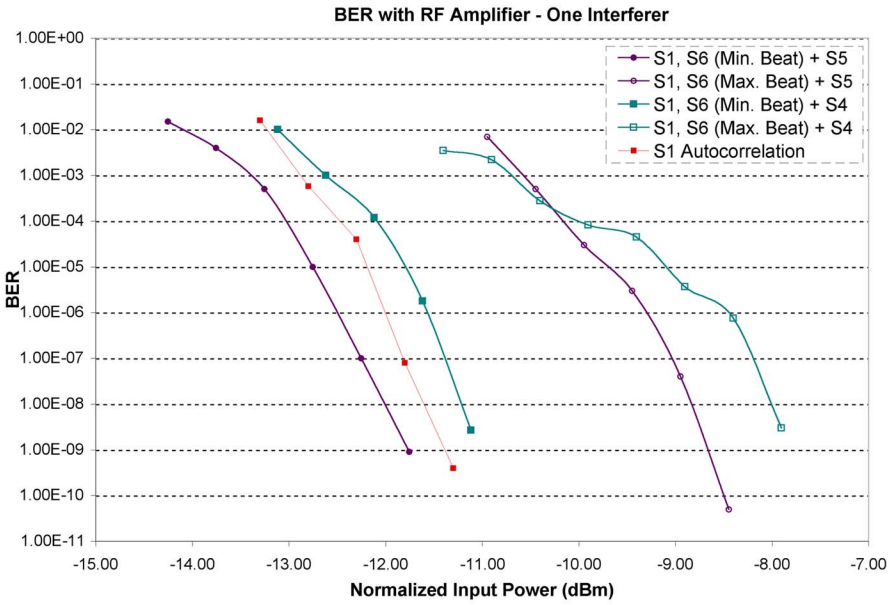

(e)

Fig. 8. Output eye diagrams for the single interferer scenario, three users on the channel, with one-chip overlap of the autocorrelation from one user and one other nonoverlapping user. (a) SPU1 and SPU6 (overlapping) and SPU5 (nonoverlapping), minimized beat noise, (b) SPU1 and SPU6 (overlapping) and SPU5 (nonoverlapping) maximized beat noise, (c) SPU1 and SPU6 (overlapping) and SPU4 (nonoverlapping) minimized beat noise, (d) SPU1 and SPU6 (overlapping) and SPU4 (nonoverlapping) maximized beat noise. (e) BER as a function of normalized received power for the single interferer scenario, three users on the channel, with one-chip overlap of the autocorrelation from one user and one other nonoverlapping user, minimized/maximized levels of beat noise; corresponding to scenarios in Figs. 8(a)–8(d).

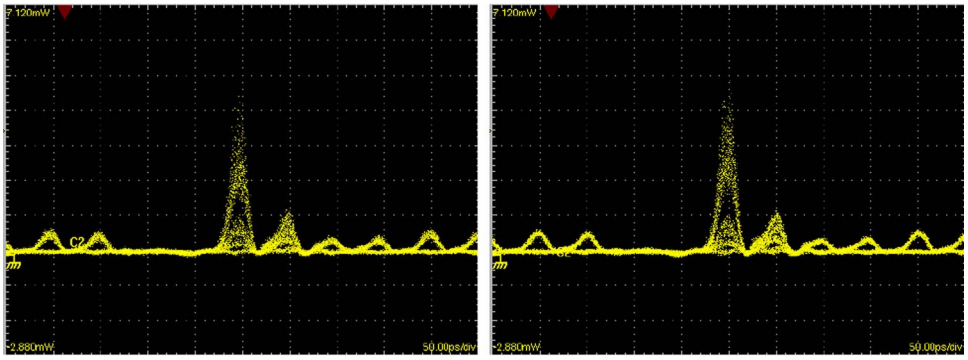

(a) (b)

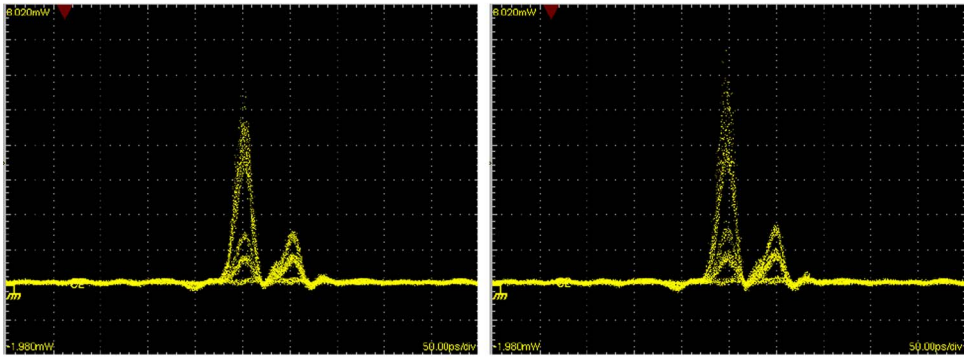

(c) (d)

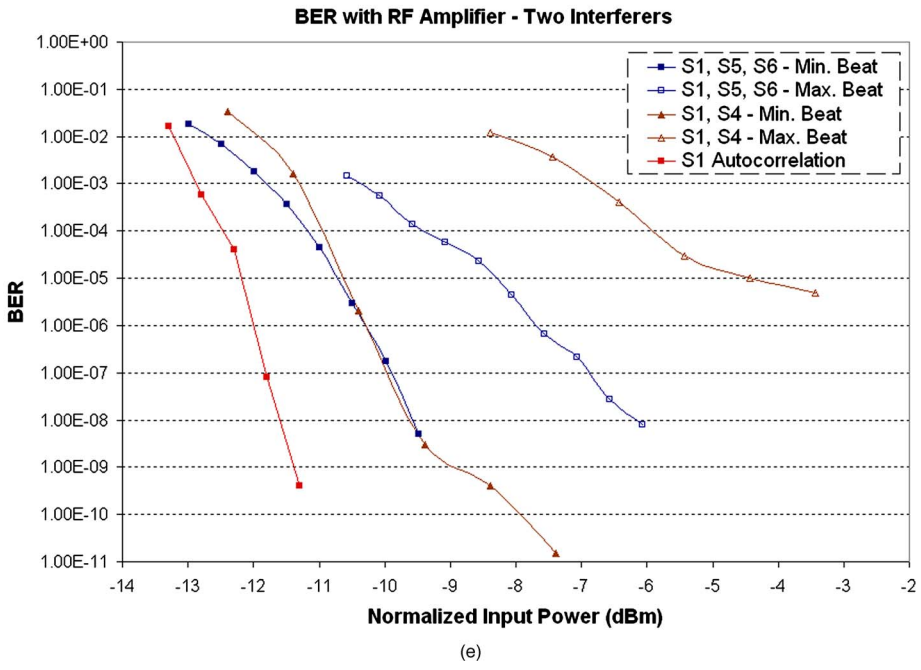

(e)

Fig. 9. Output eye diagrams for the two interferer scenario, three users on the channel, with two-chip overlap of the autocorrelation peak. (a) SPU1, SPU5, and SPU6 minimized beat noise, (b) SPU1, SPU5, and SPU6, maximized beat noise, (c) SPU1 and SPU4, minimized beat noise, (d) SPU1 and SPU4, maximized beat noise. (e) BER as a function of normalized received power for the two interferer scenario, three users on the channel, with two-chip overlap of the autocorrelation peak, minimized/maximized levels of beat noise; corresponding to scenarios in (a)–(d).

peak while the other does not. Figure 8(a) shows the eye diagram for SPU1 with SPU6 present and SPU5 not interfering with beat noise minimized. Figure 8(b) shows the eye diagram for SPU1 with SPU6 present and SPU5 not interfering, beat maximized. Similarly, Fig. 8(c) shows the eye diagram for SPU1 with SPU6 present and SPU4 not interfering, beat noise minimized and Fig. 8(d) shows the eye diagram for SPU1 with SPU6 present and SPU4 not interfering, beat noise maximized. It is important to note as a consequence of the manner in which the test bed was arranged, the presence of SPU4 as the nonoverlapping user contributes a two-chip interference (SPU5 contributes only one). The corresponding BER measurement is shown in Fig. 8(d) for these cases.

3.E. Two Interferer Scenarios

In the two interferer scenario, three users were present on the network; SPU1 and two other users whose signal interfered with SPU1. Thus two interferer chips from the cross correlation of the other users on the channel directly overlapped the SPU1 autocorrelation peak. The case of SPU1 and SPU4 was an indirectly equivalent interference from two users because the cross correlation of SPU4 was engineered to provide a level of 2. For each scenario, the minimized and maximized beat noise cases were examined.

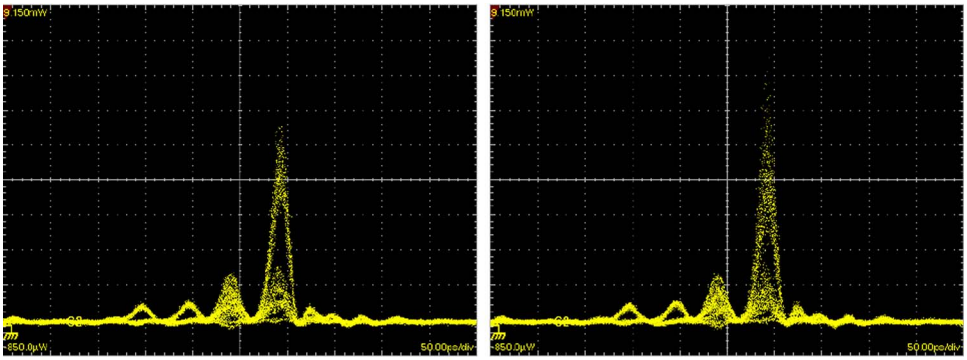

(a) (b)

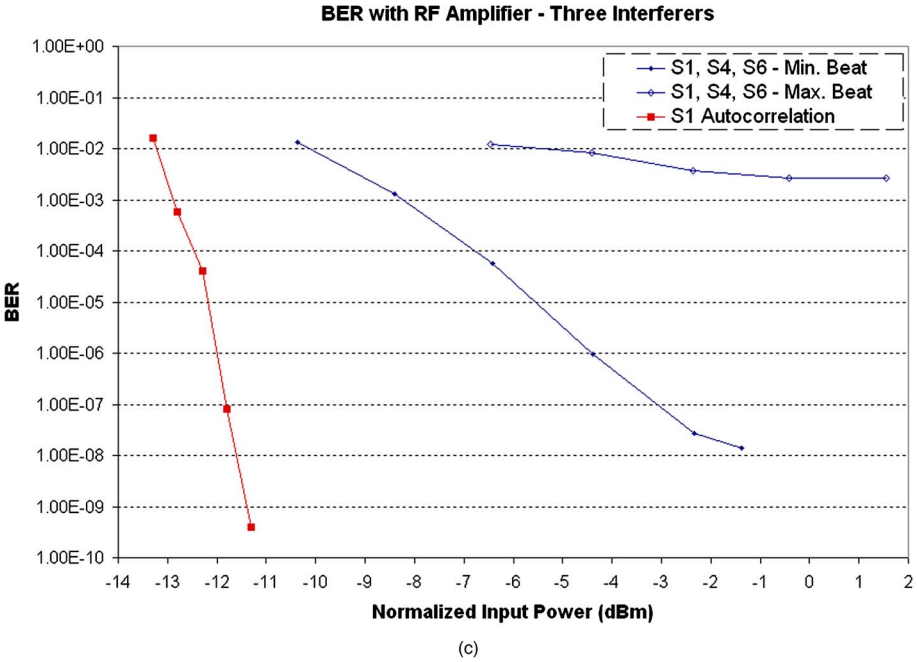

(c)

Fig. 10. Output eye diagrams for the three interferer scenario, with three-chip overlap of the autocorrelation peak (a) SPU1, SPU4, and SPU6, minimized beat noise, (b) SPU1, SPU4, and SPU6, maximized beat noise. (c) BER as a function of normalized received power for the three interferer scenario with three-chip overlap of the autocorrelation peak, minimized/maximized levels of beat noise; corresponding to scenarios in (a) and (b).

Figure 9 shows the eye diagrams for SPU1 with two other users present on the channel, i.e., an equivalent of two cross-correlation chips directly overlap the autocorrelation peak. Figure 9(a) shows the eye diagram for SPU1 with SPU5 and SPU6 present with beat noise minimized while Fig. 9(b) shows the corresponding eye diagram for SPU1 with SPU5 and SPU6 present with beat noise maximized. Figure 9(c) shows the eye diagram for SPU1 with SPU4 present, beat noise minimized. Figure 9(d) shows the eye diagram for SPU1 with SPU4 present; beat noise maximized. The BER measurements for these cases are shown in Fig. 9(e).

3.F. Three Interferer Scenario

In the three interferer scenario, three users were present on the network; SPU1, SPU4, and SPU6. The use of SPU4 produced an indirectly equivalent interference from two users because the cross correlation of SPU4 was engineered to provide a level of 2 and together with the one-chip interference contribution from SPU6 produced the desired three interferer scenario. Thus equivalently three interferer chips from the cross correlation of the other users on the channel directly overlapped the SPU1 autocorrelation peak. For each scenario, the minimized and maximized beat noise cases were examined. Figure 10 shows the eye diagram for the three interferer scenario. Figure 10(a) shows the eye diagram for SPU1 with SPU4 and SPU6, beat noise minimized. Figure 10(b) shows the eye diagram for SPU1 with SPU4 and SPU6, beat noise maximized. The BER measurements for these cases is shown in Fig. 10(c).

3.G. Interferers Only, No Overlap

It is important to note that beat noise is not only generated between the main signal and the interfering terms but also between interfering terms. The latter also play a role in overall network performance and under many scenarios contribute to the BER. Thus this set of measurements investigates the errors caused by the interferers solely, with no overlap of the autocorrelation peak.

The following scenarios have been engineered to realize interference conditions between interferers only. Figure 11 shows the eye diagrams for interferer–interferer overlap scenarios. Figure 11(a) shows the eye diagram for SPU1 with overlap of SPU4 and SPU6, beat noise minimized. Figure 11(b) shows the eye diagram for SPU1 with

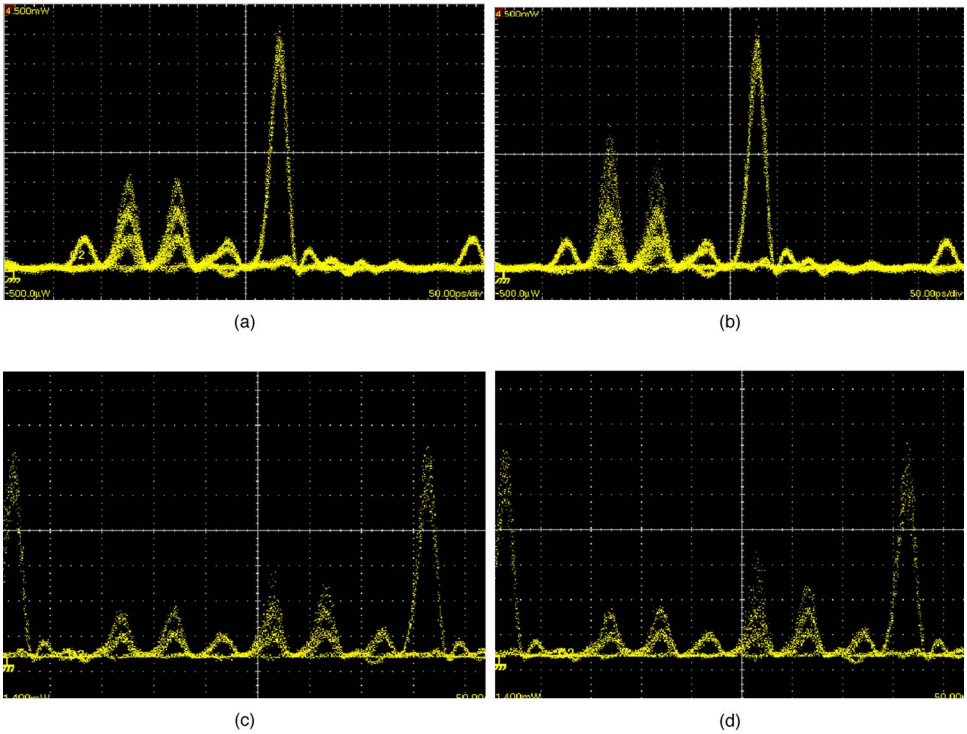

Fig. 11. Output eye diagrams for overlaps between interferers only. (a) SPU1, SPU4, and SPU6, minimized beat noise, (b) SPU1, SPU4, and SPU6, maximized beat noise, (c) SPU1 with SPU4, SPU5, and SPU6, minimized beat noise, (d) SPU1 with SPU4, SPU5, and SPU6, maximized beat noise.

overlap of SPU4 and SPU6, beat noise maximized. This scenario is equivalent to the three interferer overlap scenario, since SPU4 contributes a level of 2 chips. Figure 11(c) shows the eye diagram for SPU1 with an overlap of SPU4, SPU5, and SPU6, beat noise minimized. Figure 11(d) shows the eye diagram for SPU1 with an overlap of SPU4, SPU5, and SPU6, beat noise maximized. This scenario is equivalent to a four interferer overlap scenario.

Figure 11(c) shows BER as a function of normalized received power for interferer–interferer overlap scenarios, minimized to maximized levels of beat noise; corresponding to scenarios in Figs. 11(a)–11(d).

4. Conclusions

Beat noise has been evaluated experimentally at a data rate of 2.5 Gbits/s for 2-D TW OCDMA codes. A series of BER measurements were undertaken under a range of emulated interference conditions. The experiments have been engineered to investigate the influence of beat noise components in a representative 2-D TW OCDMA architecture. This is not representative of an extensive implementation since only four codes were used. The following must be noted at the beginning of any conclusion.

- The measured power penalties represent the worst case of aligned polarizations and complete overlap of the interfering term(s) with the autocorrelation peak.
- The power levels of the interfering signals are lower than the main signal to enable the noise process to be studied over a wider range.

The more practical scenarios that yield the exact power penalties will be a strong function of traffic statistics and network architectures. Nevertheless the results have provided clear experimental evidence that beat noise is indeed a key limiting factor.

In summary, within experimental error, the average power penalties as a function of the number of interferers are

- One interferer, no overlap; negligible.
- One interferer, with one-chip overlap; between 2–3 dB max and <1 dB min;
- one interferer, with one-chip overlap from one user and no overlap from another; between 2–3 dB max and <1 dB min;
- two interferers with two chip overlap (from two different users SPU5, SPU6); 5 dB max and 1 dB min;
- two interferers with two-chip overlap (from a single SPU4); 7 dB max and 1 dB min;
- Three interferers with three-chip overlap; error floor max and 10 dB min;
- Interferers only; negligible for both max and min.

Thus for a scenario where the interferers are ~3 dB lower in total power to that of the desired user, results indicate that this form of noise can introduce a significant power penalty at a BER of 10^{-9}:

- for a single user with nonoverlapping interferers; no significant power penalty;
- for a single interferer, 2 dB max and 0.5 dB min;
- for two interferers, 6 dB max, 2 dB min;
- for three interferers, error floor and 8 dB min;
- for the case where only the interferers are overlapping; no significant power penalty for both max and min.

As expected, the data confirm that the level of beat noise generated is a function of cochannel interference power level, which in this case is manifest through an increase in the number of interfering users overlapping with the autocorrelation peak.

Multiple user interference in all optical networks has been extensively analyzed in the open literature. The results of these analyses generally predict interference power penalties that are lower than has been observed here. However, existing theoretical models utilize a Gaussian approximation to describe the interference process, proven to be valid for large numbers of interferers (more than five). The interference scenarios reported here do not conform well to the above theoretical framework and con-

sequently the errors associated with the experiment are larger than might be expected. Nonetheless mainstream interference analysis suggest that interference levels of −10 dB for a single user will produce a power penalty of ~3 dB. This is broadly consistent with the experimental evidence provided here [25].

References

1. J. O'Reilly and C. Appleton, "System performance implications of homodyne beat noise affects in optical fiber networks," IEE Proc.: Optoelectron. **142**, 143–148 (1995).
2. P. J. Legg, M. Tur, and I. Andonovic, "Solution paths to limit interferometric noise induced performance degradation in ASK/direct detection lightwave networks," J. Lightwave Technol. **14**, 1943–1954 (1996).
3. J. Attard, J. Mitchell, and C. Rasmussen, "Performance analysis of interferometric noise due to unequally powered interferers in optical networks," J. Lightwave Technol. **23**, 1692–1703 (2005).
4. Y. Shen, K. Lu, and W. Gu, "Coherent and incoherent crosstalk in WDM optical networks," J. Lightwave Technol. **17**, 759–764 (1999).
5. T. Kamalakis and T. Spicopoulos, "Asymptotic behavior of in-band crosstalk noise in WDM networks," IEEE Photon. Technol. Lett. **15**, 476–478 (2003).
6. J. Zhang, M. Yao, Q. Xu, H. Zhang, C. Peng, and Y. Gao, "Interferometric noise in optical time division multiplexing transmission system," J. Lightwave Technol. **20**, 1329–1334 (2002).
7. P. Legg, D. K. Hunter, I. Andonovic, and P. E. Barnsley, "Inter-channel crosstalk phenomena in optical time division multiplexed switching networks," IEEE Photon. Technol. Lett. **6**, 661–663 (1994).
8. C. Desem, "Optical interference in lightwave subcarrier multiplexing systems employing multiple optical carriers," Electron. Lett. **24**, 50–51 (1988).
9. S. Soerensen, "Optical beat noise suppression and power equalization in subcarrier multiple access passive optical networks by downstream feedback," J. Lightwave Technol. **18**, 1337–1347 (2000).
10. E. Smith, P. Gough, and D. Taylor, "Noise limits of optical spectral-encoding CDMA systems," Electron. Lett. **31**, 1469–1470 (1995).
11. E. Smith, R. Blaikie, and D. Taylor, "Performance enhancement of spectral-amplitude coding optical CDMA using pulse position modulation," IEEE Trans. Power Deliv. **46**, 1176–1185 (1998).
12. Z. Wei, H. Shalaby, and H. Ghafouri-Shiraz, "Modified quadratic congruence codes for fiber Bragg grating based spectral amplitude coding optical CDMA systems," J. Lightwave Technol. **19**, 1274–1281 (2001).
13. K. Kamakura and I. Sasase, "Reduction of optical beat interference in optical frequency hopping CDMA networks using coherent multiplexing," in *Proceedings of the IEEE International Conference on Communications* (IEEE, 2001), pp. 695–700.
14. T. Demeechai and A. Sharma, "Beat noise in a non-coherent optical CDMA system," in *Proceedings of the 8th International Conference on Communication Systems (ICCS 2002)*, (IEEE, 2002), pp. 899–902.
15. G. J. Pendock and D. Sampson, "Capacity of coherence-multiplexed CDMA networks," Opt. Commun. **143**, 109–117 (1997).
16. Xu Wang and K. Kitayama, "Analysis of beat noise in coherent and incoherent time-spreading OCDMA," J. Lightwave Technol. **22**, 2226–2235 (2004).
17. L. Tančevski and L. Rusch, "Impact of the beat noise on the performance of 2-D optical CDMA systems," IEEE Commun. Lett. **4**, 264–266 (2000).
18. M. Meenakshi and I. Andonovic, "Effect of physical layer impairments on SUM and AND detection strategies for 2-D optical CDMA," IEEE Photon. Technol. Lett. **17**, 1112–1114 (2005).
19. T. Bazan, D. Harle, I. Andonovic, and M. Meenakshi, "The effect of beat noise on the performance of 2-D time spreading/wavelength hopping optical CDMA systems," J. Opt. Netw. **4**, 121–129 (2005).
20. T. Bazan, D. Harle, and I. Andonovic, "Impact of beat noise on balanced detection for 2-D time-wavelength OCDMA systems," presented at The Fourth IASTED Conference on Communication Systems and Networks (CSN 2005), Benidorm, Spain, 12–14 September 2005.
21. S. Ayott and L. Rush, "Experimental comparison of coherent versus incoherent sources in a four-user λ-t OCDMA system at 1.25 Gb/s," IEEE Photon. Technol. Lett. **17**, 2493–2495 (2005).
22. G.-C. Yang and W. Kwong, *Prime Codes With Applications to CDMA Optical and Wireless Networks* (Artech House, 2002).
23. A. Stock and E. Sargent, "Comparison of diverse optical CDMA codes using a normalized throughput metric," IEEE Commun. Lett. **7**, 242–244 (2003).
24. A. Stock and H. Sargent, "System comparison of optical CDMA and WDMA in a broadband local area network," IEEE Commun. Lett. **6**, 409–411 (2002).
25. T. Bazan, D. Harle, and I. Andonovic, "Performance analysis of 2-D time wavelength OCDMA wavelength-aware receiver with beat noise," in *Proceedings of the 2006 International Conference on Transparent Optical Networks* (IEEE, 2006), paper Th B16.